

Di- and Tricobalt Dawson Sandwich Complexes: Synthesis, Spectroscopic Characterization, and Electrochemical Behavior of $\text{Na}_{18}[(\text{NaOH}_2)_2\text{Co}_2(\text{P}_2\text{W}_{15}\text{O}_{56})_2]$ and $\text{Na}_{17}[(\text{NaOH}_2)\text{Co}_3(\text{H}_2\text{O})(\text{P}_2\text{W}_{15}\text{O}_{56})_2]$

Laurent Ruhlmann,^{*,†} Jacqueline Canny,[‡] Roland Contant,[‡] and René Thouvenot^{*,‡}

Laboratoire de Chimie Physique, Groupe TEMiC, Equipe d'Electrochimie et de Photoelectrochimie, UMR 8000, Université Paris-sud, Bâtiment 420, 91405 Orsay Cedex, France, and Laboratoire de Chimie Inorganique et Matériaux Moléculaires, UMR 7071, Case Courrier 42, Université Pierre et Marie Curie, 4, Place Jussieu, 75252 Paris Cedex 05, France

Received February 22, 2002

The reaction of the trivacant Dawson anion $\alpha\text{-}[\text{P}_2\text{W}_{15}\text{O}_{56}]^{12-}$ and the divalent cations Co^{2+} is known to form the tetracobalt sandwich complex $[\text{Co}_4(\text{H}_2\text{O})_2(\text{P}_2\text{W}_{15}\text{O}_{56})_2]^{16-}$ ($\text{Co}_4\text{P}_4\text{W}_{30}$). Two new complexes, with different $\text{Co}/\text{P}_2\text{W}_{15}$ stoichiometry, $[(\text{NaOH}_2)_2\text{Co}_2(\text{P}_2\text{W}_{15}\text{O}_{56})_2]^{18-}$ ($\text{Na}_2\text{Co}_2\text{P}_4\text{W}_{30}$) and $[(\text{NaOH}_2)\text{Co}_3(\text{H}_2\text{O})(\text{P}_2\text{W}_{15}\text{O}_{56})_2]^{17-}$ ($\text{NaCo}_3\text{P}_4\text{W}_{30}$), have been synthesized as aqueous-soluble sodium salts, by a slight modification of the reaction conditions. Both compounds were characterized by IR, elemental analysis, and ^{31}P solution NMR spectroscopy. These species are "lacunary" sandwich complexes, which add Co^{2+} cations according to $\text{Na}_2\text{Co}_2\text{P}_4\text{W}_{30} + \text{Co}^{2+} \rightarrow \text{NaCo}_3\text{P}_4\text{W}_{30} + \text{Na}^+$ followed by $\text{NaCo}_3\text{P}_4\text{W}_{30} + \text{Co}^{2+} \rightarrow \text{Co}_4\text{P}_4\text{W}_{30} + \text{Na}^+$. A Li^+/Na^+ exchange in the cavity was evidenced by ^{31}P dynamic NMR spectroscopy. The electrochemical behaviors of the sandwich complexes $[(\text{NaOH}_2)\text{Co}_3(\text{H}_2\text{O})(\text{P}_2\text{W}_{15}\text{O}_{56})_2]^{17-}$ and $[(\text{NaOH}_2)_2\text{Co}_2(\text{P}_2\text{W}_{15}\text{O}_{56})_2]^{18-}$ were investigated in aqueous solutions and compared with that of $[\text{Co}_4(\text{H}_2\text{O})_2(\text{P}_2\text{W}_{15}\text{O}_{56})_2]^{16-}$. These complexes showed an electrocatalytic effect on nitrite reduction.

Introduction

The ability to modify the redox and chemical properties of heteropolyanions by replacing one or many elements renders them particularly attractive for catalytic and electrocatalytic applications.¹ For instance, the Dawson $[\text{P}_2\text{W}_{18}\text{O}_{62}]^{6-}$ polyoxoanion may be hydrolyzed into lacunary complexes containing one ($\alpha_2\text{-}[\text{P}_2\text{W}_{17}\text{O}_{61}]^{10-}$), three ($\alpha\text{-}[\text{P}_2\text{W}_{15}\text{O}_{56}]^{12-}$), or six vacant sites ($\alpha\text{-}[\text{H}_2\text{P}_2\text{W}_{12}\text{O}_{48}]^{12-}$).² It is

well-known that the reaction of $\alpha\text{-}[\text{P}_2\text{W}_{15}\text{O}_{56}]^{12-}$ with transition metal cations yields two kinds of derivatives: (i) $[\text{M}_3\text{P}_2\text{W}_{15}\text{O}_{62}]^{n-}$ ($\text{M} = \text{Ti}^{\text{IV}}, \text{Zr}^{\text{IV}}, \text{Hf}^{\text{IV}}, \text{V}^{\text{V}}, \text{Nb}^{\text{V}}, \text{Ta}^{\text{V}}, \text{Mo}^{\text{VI}}, \text{W}^{\text{VI}}$), where M substitutes for W,³ and (ii) $[\text{M}_4(\text{H}_2\text{O})_2(\text{P}_2\text{W}_{15}\text{O}_{56})_2]^{n-}$ ($\text{M} = \text{Mn}^{\text{II}}, \text{Fe}^{\text{III}}, \text{Co}^{\text{II}}, \text{Ni}^{\text{II}}, \text{Cu}^{\text{II}}, \text{Zn}^{\text{II}}, \text{and Cd}^{\text{II}}$), where a sheet of four M atoms are sandwiched between two P_2W_{15} subunits.^{4–6} A third class of Dawson derivatives has been recently discovered with the full characterization of the dinuclear sandwich compound $[(\text{NaOH}_2)_2\text{Fe}_2(\text{P}_2\text{W}_{15}\text{O}_{56})_2]^{16-}$.^{6–7}

* To whom correspondence should be addressed. E-mail: rth@ccr.jussieu.fr (R.T.); laurent-ruhlmann@lcp.u-psud.fr (L.R.).

[†] Université Paris-sud, Orsay.

[‡] Université Pierre et Marie Curie, Paris.

- (1) (a) Keita, B.; Nadjjo, L.; Contant, R.; Fournier, M.; Hervé, G. French Patent (CNRS) 8911, 728, February 10, 1989. (b) Keita, B.; Nadjjo, L.; Contant, R.; Fournier, M.; Hervé, G. Eur. Patent (CNRS), Appl. EP 382,644; *Chem. Abstr.* **1991**, *114*, 191882u. (c) Keita, B.; Belhouari, A.; Nadjjo, L.; Contant, R. *J. Electroanal. Chem.* **1995**, *181*, 243. (d) Abbessi, M.; Contant, R.; Thouvenot, R.; Hervé, G. *Inorg. Chem.* **1991**, *30*, 1695. (e) Keita, B.; Eassadi, K.; Nadjjo, L.; Contant, R.; Justum, Y. *J. Electroanal. Chem.* **1996**, *404*, 271. (f) McGarvey, J. F.; Pope, M. T. *Inorg. Chem.* **1978**, *17*, 1115. (g) Keita, B.; Lu, Y. W.; Nadjjo, L.; Contant, R.; Abbessi, M.; Canny, J.; Richet, M. *J. Electroanal. Chem.* **1999**, *477*, 146.
- (2) (a) Ciabrini, J. P.; Contant, R.; Fruchart, J.-M. *Polyhedron* **1983**, *2*, 1229. (b) Contant, R.; Ciabrini, J. P. *J. Chem. Res., Synop.* **1977**, 222; *J. Chem. Res., Miniprint* **1977**, 2601. (c) Contant, R. *Inorg. Synth.* **1990**, *27*, 104.

- (3) (a) Finke, R. G.; Rapko, B.; Saxton, R. J.; Domaille, P. J. *J. Am. Chem. Soc.* **1986**, *108*, 2947. (b) Meng, L.; Liu, J. F. *Chin. Chem. Lett.* **1994**, *6*, 547. (c) Pope, M. T. *Heteropoly and Isopoly Oxometalates*; Springer-Verlag: Berlin, 1983.
- (4) (a) Finke, R. G.; Droegge, M. W. *Inorg. Chem.* **1983**, *22*, 1006. (b) Finke, R. G.; Droegge, M. W.; Domaille, P. J. *Inorg. Chem.* **1987**, *26*, 3886. (c) Weakley, T. J. R.; Finke, R. G. *Inorg. Chem.* **1990**, *29*, 1235. (d) Ciabrini, J.-P.; Contant, R. *J. Chem. Res., Synop.* **1993**, 391; *J. Chem. Res., Miniprint* **1993**, 2719. (e) Gómez-García, C. J.; Borrás-Almenar, J. J.; Coronado, E.; Ouahab, L. *Inorg. Chem.* **1994**, *33*, 4016. (f) Finke, R. G.; Weakley, T. J. R. *J. Chem. Cryst.* **1994**, *24*, 123. (g) Kirby, J. F.; Baker, L. C. W. *J. Am. Chem. Soc.* **1995**, *117*, 10010. (h) Crano, N. J.; Chambers, R. C.; Lunch, V. M.; Fox, M. A. *J. Mol. Catal. A: Chem.* **1996**, *114*, 65. (i) Zhang, X.; Duncan, D. C.; Campana, C. F.; Hill, C. L. *Inorg. Chem.* **1997**, *36*, 4208. (j) Müller, A.; Peter, F.; Pope, M.; Gatteschi, D. *Chem. Rev.* **1998**, *98*, 239. (k) Meng, L.; Liu, J. F. *Chem. Res. Chin. Univ.* **1998**, *14*, 1. (l) Zhang, X.; Hill, C. L. *Chem. Ind. (London)* **1998**, *75*, 519.

An analogous structure has also been recently reported by Pope and co-workers starting from the lacunary Keggin anion $[A-PW_9O_{34}]^{9-}$; actually, the reaction of $Na_9[A-PW_9O_{34}]$ with $UO_2(NO_3)_2$ gives $[Na_2(UO_2)_2(PW_9O_{34})_2]^{12-}$, which is the first reported example of a sandwich species incorporating two hetero metals.⁸

The sandwich complexes can be used in catalytic reaction as inorganic analogues of metalloporphyrin with the advantage of being more robust in an oxidizing environment and more thermally stable than complexes based on organic ligands.⁹ Moreover, Dawson-type sandwich complexes containing two (or three) transition metal atoms appear even more interesting as the two (or three) central metal ions can be varied considerably and mixed sandwich complexes might be obtained by simple addition reactions. With the aim of extending these new series to other interesting sandwich complexes, we report here for the first time the synthesis and the full characterization by IR, ^{31}P NMR spectroscopy, and elemental analysis of the di- and tricobalt sandwich type tungstophosphates $[(NaOH)_2Co_2(P_2W_{15}O_{56})_2]^{18-}$ (shortly $Na_2Co_2P_4W_{30}$) and $[(NaOH)_2Co_3(H_2O)(P_2W_{15}O_{56})_2]^{17-}$ (shortly $NaCo_3P_4W_{30}$). We present also the electrochemical behavior of $Na_2Co_2P_4W_{30}$ and $NaCo_3P_4W_{30}$ in comparison with that of the tetracobalt complex $[Co_4(H_2O)_2(P_2W_{15}O_{56})_2]^{16-}$ (shortly $Co_4P_4W_{30}$). The catalytic effect on nitrite reduction is also reported.

Experimental Section

General Comment. Most common laboratory chemicals were reagent grade, purchased from commercial sources and used without further purification.

Preparation of compounds. The potassium salt of α - $[P_2W_{18}O_{62}]^{6-}$ and the sodium salt of α - $[P_2W_{15}O_{56}]^{12-}$ were prepared by published methods.² The tetranuclear Dawson-derived sandwich complex $[Co_4(H_2O)_2(P_2W_{15}O_{56})_2]^{16-}$ was prepared as described previously.⁷

$Na_{18}[Na_2Co_2(P_2W_{15}O_{56})_2] \cdot 57H_2O$ (1) and $Na_{17}[NaCo_3(P_2W_{15}O_{56})_2] \cdot 48H_2O$ (2). These complexes were obtained in the same synthetic procedure as follows: $Co(NO_3)_2 \cdot 6H_2O$ (0.68 g; 2.34 mmol) was dissolved in 100 mL of a 2 M NaCl aqueous solution. α - $Na_{12}P_2W_{15}O_{56} \cdot 24H_2O$ (10.00 g; 2.26 mmol) was then added with vigorous stirring. The solution was heated at 40 °C until complete dissolution (~15 min). The solution was filtered hot and was left in the air. On cooling, a pale pink powder appeared immediately, and the precipitation continued for 2 h. This first fraction (compound (1)) was collected on a sintered glass frit and air-dried under water pump for 3 h (yield: 6.24 g of crude product). The filtrate was left in opened vessel, and tiny dark-violet crystals (compound (2)) appear after ~2 days; they were collected on a sintered glass frit after 4 days and dried in air (yield: 3.87 g).

Compound 1 was recrystallized from 350 mL of 0.5 M NaCl aqueous solution. The pink crystals of $Na_{20}Co_2P_4W_{30}O_{112} \cdot 57H_2O$ were filtered and dried in air (yield 4.20 g, 0.466 mmol, 41.2%).

Anal. Calcd for $Na_{20}Co_2P_4W_{30}O_{112} \cdot 57H_2O$: Co, 1.31; P, 1.37; W, 61.04; H_2O , 11.36. Found: Co, 1.36; P, 1.35; W, 60.13; H_2O , 11.30.

^{31}P NMR in D_2O/H_2O (1:1) shows 2 peaks at $\delta = -4.2$ ppm (P(2); $\Delta\nu_{1/2} = 10$ Hz) and +299 ppm (P(1); $\Delta\nu_{1/2} = 300$ Hz).

Compound 2 was also recrystallized from 150 mL of 2 M NaCl aqueous solution. The dark-violet crystals of $Na_{18}Co_3P_4W_{30}O_{112} \cdot 48H_2O$ were filtered and dried in air (yield: 2.80 g, 0.308 mmol, 27.3%).

Anal. Calcd for $Na_{18}Co_3P_4W_{30}O_{112} \cdot 48H_2O$: Co, 1.99; P, 1.39; W, 62.06; H_2O , 9.73. Found: Co, 1.96; P, 1.35; W, 60.45; H_2O , 9.73.¹⁰

Purity was ascertained by ^{31}P NMR in D_2O/H_2O (1:1), which shows two sets of two peaks at $\delta = -9.3$ and +22.0 ppm ($\Delta\nu_{1/2} = 10$ Hz) and at $\delta = +1125$ and +1673 ppm ($\Delta\nu_{1/2} = 450$ Hz).

NMR and IR Measurements. ^{31}P NMR spectra were recorded in 5 mm o.d. tubes on a Bruker AC 300 apparatus operating at 121.5 MHz in a Fourier transform mode (equipped with a QNP probe for ^{31}P NMR). The ^{31}P chemical shifts were measured at 300 K on 0.02 M solutions of the polyanions in aqueous D_2O/H_2O (1:1) solution and were referenced to external 85% H_3PO_4 (IUPAC convention) by the substitution method.

IR spectra were recorded on a Bio-Rad FTS 165 FTIR spectrophotometer on KBr pellets.

Electrochemical Experiments. Water used for all electrochemical measurements was obtained by passing through a Milli-RO4 unit and subsequently through a Millipore Q water purification set. H_2SO_4 solutions and solid Na_2SO_4 were commercial products (Prolabo). The electrolyte was made up from 0.5 M Na_2SO_4 aqueous solution, and its pH was precisely adjusted to 2.52 by addition of 0.5 M ($H_2SO_4 + Na_2SO_4$) aqueous solution. Other pHs were adjusted by addition of either H_2SO_4 or NaOH (Prolabo). The solutions were deaerated thoroughly for at least 30 min by bubbling argon (Ar-U from Air Liquide) and kept under argon atmosphere during the whole experiment.

The source, mounting, and polishing of the glassy carbon (GC, Tokai, Japan) have been described previously.¹¹ The glassy carbon samples had a diameter of 3 mm. The electrochemical setup was an EG&G 273A driven by a PC with 270 software. Potentials are quoted against a saturated calomel electrode (SCE). The counter electrode was a platinum gauze of large surface area. All voltametric experiments were carried out at room temperature.

Analyses. Elemental analyses were performed by classical gravimetric, potentiometric, and spectroscopic methods.

The anions were preliminary decomposed in boiling concentrated hydrochloric acid solution. Then W and P were precipitated together by adding cinchonium hydrochloride. Tungsten and phosphorus were determined simultaneously as WO_3 and P_2O_5 by gravimetry

(5) Song, W. B.; Wang, X. H.; Liu, Y.; Liu, J. F.; Xu, H. D. *J. Electroanal. Chem.* **1999**, *479*, 85.

(6) (a) Zhang, X.; Anderson, T. M.; Chen, Q.; Hill, C. L. *Inorg. Chem.* **2001**, *40*, 418–419. (b) Anderson, T. M.; Hardcastle, K. I.; Okun, N.; Hill, C. L. *Inorg. Chem.* **2001**, *40*, 6418.

(7) Ruhlmann, L.; Nadjo, L.; Canny, J.; Contant, R.; Thouvenot, R. *Eur. J. Inorg. Chem.* **2002**, 975.

(8) Kim, K.-C.; Pope, M. T. *J. Am. Chem. Soc.* **1999**, *121*, 8512.

(9) (a) Lyon, D. K.; Miller, W. K.; Novet, T.; Domaille, P. J.; Evitt, E.; Johnson, D. C.; Finke, R. G. *J. Am. Chem. Soc.* **1991**, *113*, 7209. (b) Mansuy, D.; Bartoli, J. F.; Lyon, D. K.; Finke, R. G. *J. Am. Chem. Soc.* **1991**, *113*, 7222–7226.

(10) For W content, deviations between calculated and experimental values may exceed 1%, especially for transition-metal-containing POMs, even when identity and purity of the species are not questionable. For example, in ref 9a, two W analyses of the same manganese derivative of the monovacant Dawson anion α_2 - $[(n-C_4H_9)_4N]_{7.3}H_{0.7}P_2W_{17}O_{61}(Mn^{3+} \cdot Br)]$ are reported which differ from more than 1% (50% and 51.4%, respectively, for a calculated value of 51.5%). The discrepancy is even worse for a Co-containing tungstoarsenate $Na_{12}[As_2W_{18}\{Co(H_2O)\}_3O_{56}] \cdot 34H_2O$ for which deviation between calculated (58.74%) and experimental (61.22%) amounts to nearly 2.5%. See: Mialane, P.; Marrot, T.; Rivière, E.; Nebout, J.; Hervé, G. *Inorg. Chem.* **2001**, *40*, 44.

(11) Keita, B.; Essaadi, K.; Nadjo, L. *Electroanal. Chem. Interfacial Electrochem.* **1989**, *259*, 127.

after calcination of the cinchonium salt. Cobalt which remained in the filtrate was complexed with ammonia as $\text{Co}(\text{NH}_3)_6^{3+}$ and then titrated by potentiometry with hexacyanoferrate(III). Phosphorus was determined independently by spectroscopy of the molybdo-vanadophosphate.¹² Water content was determined by thermogravimetric analysis.

Results and Discussion

Synthesis. This study allowed us to obtain in a controlled manner two new sandwich complexes of low cobalt nuclearity with respect to well-known tetracobalt species $[\text{Co}_4(\text{H}_2\text{O})_2(\text{P}_2\text{W}_{15}\text{O}_{56})_2]^{16-}$ ($\text{Co}_4\text{P}_4\text{W}_{30}$), that is $[(\text{H}_2\text{O})_2\text{NaCo}_3(\text{P}_2\text{W}_{15}\text{O}_{56})_2]^{17-}$ ($\text{NaCo}_3\text{P}_4\text{W}_{30}$) and $[(\text{NaOH}_2)_2\text{Co}_2(\text{P}_2\text{W}_{15}\text{O}_{56})_2]^{18-}$ ($\text{Na}_2\text{Co}_2\text{P}_4\text{W}_{30}$). The procedures described in the Experimental Section were rationalized thanks to the systematic investigation of various synthetic mixtures by ³¹P NMR. Whatever the relative concentration of the reagents (Co^{II} and P_2W_{15}), low pH favors the formation of the symmetrical tetranuclear cluster $\text{Co}_4\text{P}_4\text{W}_{30}$. This compound is the only one which can be obtained as a pure species, from acidic solution.⁷ The formation of the two other species requires a neutral medium, but neither of them can be obtained directly as pure compound: depending on the $\text{Co}/\text{P}_2\text{W}_{15}$ stoichiometry, they are present in binary mixtures containing either $\text{Na}_2\text{Co}_2\text{P}_4\text{W}_{30}$ and $\text{NaCo}_3\text{P}_4\text{W}_{30}$, or $\text{NaCo}_3\text{P}_4\text{W}_{30}$ and $\text{Co}_4\text{P}_4\text{W}_{30}$. Using 1.5 equiv of Co^{II} leads to a 1/3 mixture of $\text{Co}_4\text{P}_4\text{W}_{30}$ and $\text{NaCo}_3\text{P}_4\text{W}_{30}$. However, because the two compounds have nearly the same solubility, the trinuclear species $\text{NaCo}_3\text{P}_4\text{W}_{30}$ could not be isolated from the solution. By systematically varying the experimental conditions, especially the $\text{Co}/\text{P}_2\text{W}_{15}$ ratio, we found that an optimal yield in both $\text{Na}_2\text{Co}_2\text{P}_4\text{W}_{30}$ and $\text{NaCo}_3\text{P}_4\text{W}_{30}$, avoiding formation of $\text{Co}_4\text{P}_4\text{W}_{30}$, required the use of a slight excess of Co^{II} with respect to the 1/1 ratio and that the syntheses had to be performed in neutral medium and at high Na^+ (2 M) concentration. The low solubility of the sodium salt of the dicobalt complex allows its separation by precipitation from the synthetic mixture. Pure $\text{NaCo}_3\text{P}_4\text{W}_{30}$ and $\text{Na}_2\text{Co}_2\text{P}_4\text{W}_{30}$ are obtained by crystallization from 2 and 0.5 M NaCl aqueous solutions, respectively. These complexes were then readily prepared in high purity with ~27–41% isolated yield, respectively.

IR Characterization. The IR spectra of $\text{Na}_{18}[\text{Na}_2\text{Co}_2(\text{P}_2\text{W}_{15}\text{O}_{56})_2] \cdot 57\text{H}_2\text{O}$ and $\text{Na}_{17}[\text{NaCo}_3(\text{P}_2\text{W}_{15}\text{O}_{56})_2] \cdot 48\text{H}_2\text{O}$ are shown in Figure 1 and are compared to that of the parent compounds $\alpha\text{-Na}_{12}[\text{P}_2\text{W}_{15}\text{O}_{56}] \cdot 24\text{H}_2\text{O}$, $\alpha\text{-K}_6[\text{P}_2\text{W}_{18}\text{O}_{62}] \cdot 19\text{H}_2\text{O}$, and $\text{Na}_{16}[\text{Co}_4(\text{P}_2\text{W}_{15}\text{O}_{56})_2] \cdot 53\text{H}_2\text{O}$.

Except the $\text{W}-\text{O}$ or $\text{W}-\text{O}-\text{W}$ bands which appear at low wavenumbers ($<1000\text{ cm}^{-1}$),¹³ IR spectra of phosphorus-centered polyoxotungstates are characterized by well separated $\text{P}-\text{O}$ stretching vibrations which are observed between 1200 and 1000 cm^{-1} .¹⁴

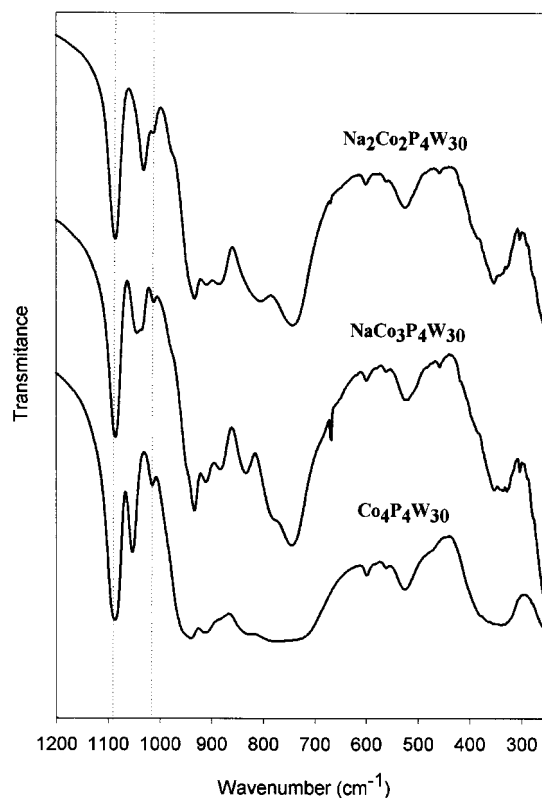


Figure 1. Comparison of the IR spectra (KBr) of the hydrated sandwich heteropolyanions $\text{Na}_2\text{Co}_2\text{P}_4\text{W}_{30}$, $\text{NaCo}_3\text{P}_4\text{W}_{30}$, and $\text{Co}_4\text{P}_4\text{W}_{30}$.

In our previous paper, we discussed in detail the pattern of the PO_4 stretching region for various Dawson-type complexes based on P_2W_{15} .⁷ For all these species, the vibration modes of the unperturbed PW_9 moiety are nearly invariant, at $\sim 1080\text{ cm}^{-1}$ (strong) and 1010 cm^{-1} (low to medium). For the perturbed subunit PW_6 , the number of IR absorption bands and their position depend on the interaction of the addenda atoms with the free oxygen (O_{ter}) of the phosphate group. Hence, the high-wavenumber band of P_2W_{15} at 1130 cm^{-1} , which can be ascribed to $\nu(\text{P}-\text{O}_{\text{ter}})$, moves to lower frequency in the sandwich complexes where the PO bond has lost its double-bond character; it corresponds to the medium-intensity band which appears between the PW_9 bands, in the range $1030\text{--}1060\text{ cm}^{-1}$.

This PW_6 moiety band is observed at 1056 cm^{-1} for $\text{Co}_4\text{P}_4\text{W}_{30}$ and at 1030 cm^{-1} for $\text{Na}_2\text{Co}_2\text{P}_4\text{W}_{30}$, but the tricobalt sandwich type tungstophosphate $\text{NaCo}_3\text{P}_4\text{W}_{30}$ shows a splitting of this phosphate band, at 1044 and 1035 cm^{-1} . All these observations could be interpreted as follows: (i) The trend to high-wavenumber shift with increasing cobalt content agrees with the progressive saturation of the lacunary species.¹⁵ (ii) The presence of two bands for the tricobalt complex instead of one band for the tetra- and dicobalt species suggests a nonsymmetrical structure with two different PW_6 units.

Actually, the tetranuclear complex consists of an oxo-aqua metallic core, $\text{Co}_4\text{O}_{14}(\text{H}_2\text{O})_2$, sandwiched between two trivalent $\text{B}-\alpha\text{-}[\text{P}_2\text{W}_{15}\text{O}_{56}]$ moieties according to C_{2h} symmetry.^{4a,b}

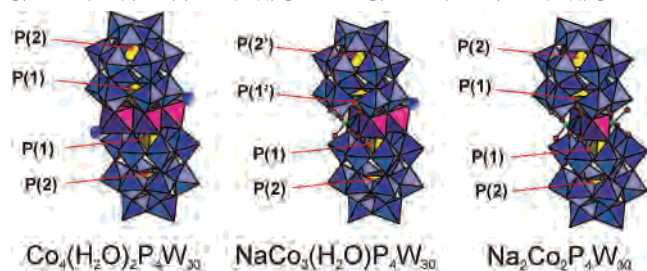
(12) Cherretton, B.; Chauveau, F.; Bertho, G.; Courtin, P. *Chim. Anal. (Paris)* **1965**, *47*, 17.

(13) Rocchiccioli-Deltcheff, C.; Thouvenot, R.; Franck, R. *Spectrochim. Acta* **1976**, *22A*, 587–597.

(14) (a) Rocchiccioli-Deltcheff, C.; Thouvenot, R. *J. Chem. Res., Synop.* **1977**, 46–47; *J. Chem. Res., Miniprint* **1977**, 549–571. (b) Rocchiccioli-Deltcheff, C.; Thouvenot, R. *Spectrosc. Lett.* **1979**, *12*, 127–138.

(15) Rocchiccioli-Deltcheff, C.; Thouvenot, R. *C. R. Acad. Sci., Ser. C* **1974**, *278*, 857–860.

Scheme 1. Proposed Structures of $[\text{Co}_4(\text{H}_2\text{O})_2(\text{P}_2\text{W}_{15}\text{O}_{56})_2]^{16-}$, $[(\text{NaOH}_2)\text{Co}_3(\text{H}_2\text{O})(\text{P}_2\text{W}_{15}\text{O}_{56})_2]^{17-}$, and $[(\text{NaOH}_2)_2\text{Co}_2(\text{P}_2\text{W}_{15}\text{O}_{56})_2]^{18-}$



The structure of dicobalt species **1** is likely to be similar to that of the diiron sandwich complex whose X-ray structure was reported by Hill and co-workers.⁶ This structure is related to that of the tetrametallic species by replacing the two “external” transition metals by two Na^+ ions; this substitution maintains the C_{2h} symmetry of the framework (Scheme 1), and therefore, there are two equivalent PW_6Co_2 “lacunary” subunits ($\nu = 1030 \text{ cm}^{-1}$). For trinuclear complex **2**, the IR spectrum shows two different PW_6Co_n subunits, likely one “saturated” PW_6Co_3 where the O_{ter} atom of the phosphate is linked to three Co atoms ($\nu = 1044 \text{ cm}^{-1}$) and one “unsaturated” PW_6Co_2 with only two Co atoms bound to O_{ter} ($\nu = 1035 \text{ cm}^{-1}$). This corresponds to a $\text{NaCo}_3\text{P}_4\text{W}_{30}$ structure where the “external” sites of the metallic core are occupied by one Na^+ and one $\text{Co}(\text{II})$ ions, which results in a symmetry of the whole complex lowered to C_s (see Scheme 1). Such a trimetallic cluster is not unprecedented: actually, as recently reported by Hill and co-workers, a central diferric-copper unit is sandwiched between two substitutionally distinct Dawson moieties in $[(\text{H}_2\text{ONa})(\text{H}_2\text{OCu})\text{Fe}_2\{(\text{P}_2\text{W}_{15}\text{O}_{56})-(\text{P}_2\text{Cu}_2(\text{H}_2\text{O})_4\text{W}_{13}\text{O}_{52})\}]^{16-}$.^{6b}

Table 1. ^{31}P NMR Data for the Cobalt Sandwich Species^a

compound	P(1) ^b		P(2) ^b	
	δ^c	$\Delta\nu_{1/2}^d$	δ^c	$\Delta\nu_{1/2}^d$
$\text{Co}_4\text{P}_4\text{W}_{30}$	1483	420	9.9	20
1	1299	300	-4.2	10
1^e	1183	700	2.5	200
2	1125	450	-9.3	10
	1673	450	22.0	10
2^e	1145 (1307)	1000 (950)	-4.7 (-6.0)	280 (120)
	1257 (1449)	1000 (700)	(-0.3)	(140)
	1411 (1624)	1000 (1200)	20.3 (28.4)	100 (160)
	1658 (1912 ^f)	1000 (^f)	(31.4)	(180)

^a Unless noted, 0.02 M solution in $\text{D}_2\text{O}/\text{H}_2\text{O}$ (1:1) measured at 300 K. ^b P(1) and P(2) in the PW_6 and PW_9 subunits, respectively. ^c In ppm with respect to 85% H_3PO_4 . ^d In Hz. ^e In $\text{D}_2\text{O}/\text{H}_2\text{O}$ (1:1) with 100 added equiv of Li^+ at 300 K and (in brackets) at 274 K. ^f Folded peak; δ recalculated, line width not significant.

^{31}P NMR Characterization. ^{31}P NMR spectroscopy is particularly suitable to check the polyoxometalate purity and to characterize the nature of the substituting elements. The ^{31}P NMR spectra for the sandwich Dawson derivatives $[\text{Co}_4(\text{H}_2\text{O})_2(\text{P}_2\text{W}_{15}\text{O}_{56})_2]^{16-}$, $[(\text{NaOH}_2)\text{Co}_3(\text{H}_2\text{O})(\text{P}_2\text{W}_{15}\text{O}_{56})_2]^{17-}$, and $[(\text{NaOH}_2)_2\text{Co}_2(\text{P}_2\text{W}_{15}\text{O}_{56})_2]^{18-}$ are reported in Figure 2, and all data are given in Table 1. Paramagnetic Dawson species always exhibit two markedly different types of ^{31}P resonances: the P atom in the perturbed subunit (numbered P(1)), which is close to the paramagnetic center(s), gives rise to broad and strongly shifted (generally to high frequency) signals, and that in the PW_9 subunit (numbered P(2)), far from the paramagnetic center(s), gives relatively sharp lines with a chemical shift close to that of diamagnetic metallophosphates (between +20 and -20 ppm).¹⁶

As for $\text{Co}_4\text{P}_4\text{W}_{30}$, the ^{31}P NMR spectrum of **1** exhibits two lines, at +1299 ppm (P(1); $\Delta\nu_{1/2} = 300 \text{ Hz}$) and -4.2

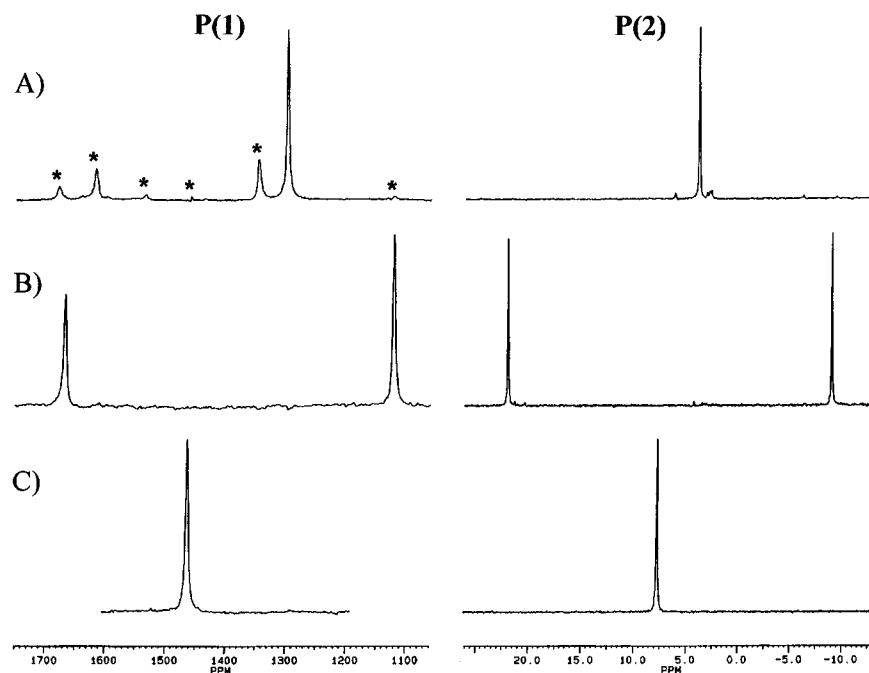


Figure 2. 121.5 MHz ^{31}P NMR spectra of $\text{Na}_2\text{Co}_2\text{P}_4\text{W}_{30}$ (A), $\text{NaCo}_3\text{P}_4\text{W}_{30}$ (B), and $\text{Co}_4\text{P}_4\text{W}_{30}$ (C). Concentration is 0.02 M in $\text{D}_2\text{O}/\text{H}_2\text{O}$ (1:1). Left: region of the P(1)s. Experimental conditions: spectral width 125 kHz; pulse width $2 \mu\text{s}$ ($\sim 40^\circ$ flip angle); 8000 data points; acquisition time 33 ms; ~ 100000 transients acquired without relaxation delay; line broadening factor 40 Hz. Right: region of the P(2)s. Experimental conditions: spectral width 9 kHz; pulse width $2 \mu\text{s}$ ($\sim 40^\circ$ flip angle); 4000 data points; acquisition time 0.23 s; ~ 1000 transients acquired without relaxation delay; line broadening factor 4 Hz. Partial degradation of $\text{Na}_2\text{Co}_2\text{P}_4\text{W}_{30}$ occurs during overnight acquisition for the P(1) region. Asterisks indicate signals from additional species.

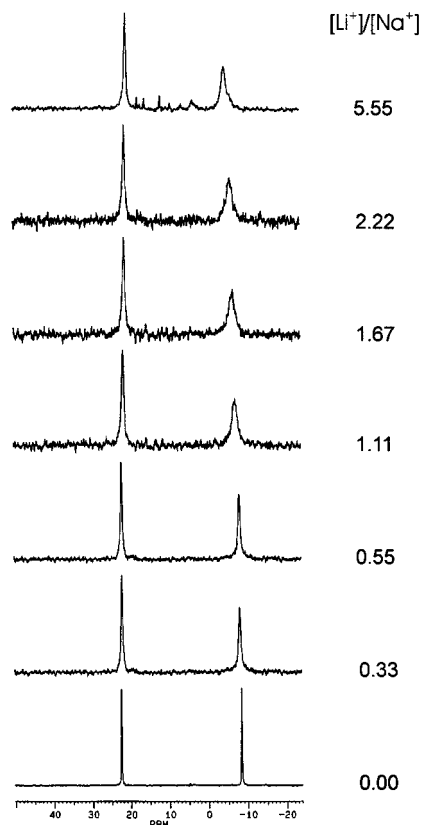


Figure 3. Low-frequency part (P(2) region) of the 121.5 MHz ^{31}P NMR spectra of $\text{NaCo}_3\text{P}_4\text{W}_{30}$ (0.02 M) in the presence of various concentrations of LiCl . Temperature: 300 K. For the other experimental conditions, see Figure 2.

ppm (P(2); $\Delta\nu_{1/2} = 10$ Hz), consistent with the equivalence of the two P_2W_{15} moieties. In contrast, **2** presents two narrow lines ($\Delta\nu_{1/2} = 10$ Hz) of equal intensity, at $\delta = -9.3$ ppm and $+22.0$ ppm assigned to P(2) and P(2') and two broad bands ($\Delta\nu_{1/2} = 450$ Hz) at $\delta = +1125$ and $+1673$ ppm attributed to P(1) and P(1') (Figure 2); this confirms that the two P_2W_{15} moieties are no more equivalent in the tricobalt species (Scheme 1).

It should be noted that ^{31}P NMR allows us to follow the stability of the various Co complexes. In aqueous solution, the spectra of $\text{Co}_4\text{P}_4\text{W}_{30}$ and $\text{NaCo}_3\text{P}_4\text{W}_{30}$ do not change with time; on the contrary, spurious lines appear in the case of $\text{Na}_2\text{Co}_2\text{P}_4\text{W}_{30}$ during the overnight acquisition required for the deshielded region (P(1)) (see Figure 2A).

At 300 K, addition of Li^+ to the aqueous solution of the Na^+ salt of **2** induces a broadening of both P(2) resonances (Figure 3). The line width increases with the Li^+ concentration up to a $[\text{Li}^+]/[\text{Na}^+]$ value of about 1. Further addition of Li^+ does not change the spectrum significantly, except small spurious signals which appear for $[\text{Li}^+]/[\text{Na}^+]$ close to 5 indicating a partial degradation of the starting species (see Figure 3).

Broadening of the NMR P(2) resonances suggests a dynamic process. This is confirmed by the variable temperature study which shows a splitting of both P(2) signals at

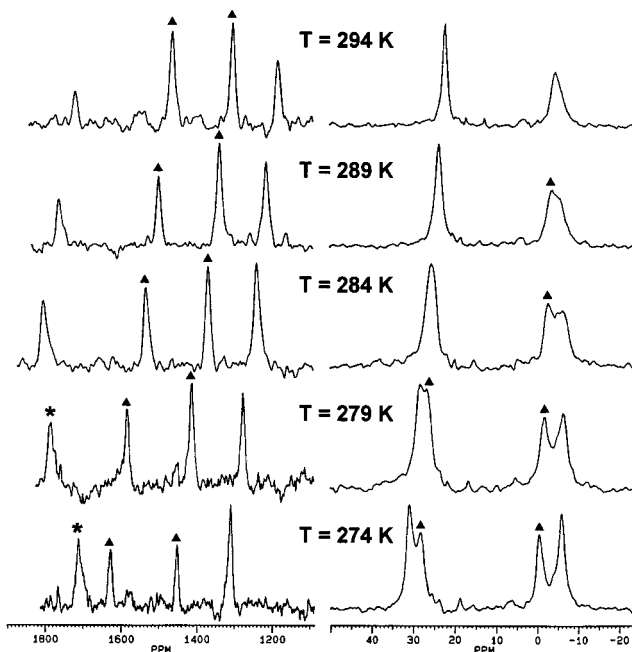


Figure 4. Variable temperature (274–294 K) ^{31}P NMR study of $[(\text{NaOH})_2\text{Co}_3(\text{H}_2\text{O})(\text{P}_2\text{W}_{15}\text{O}_{56})_2]^{17-}$ in the presence of 100 equiv of Li^+ . The symbol \blacktriangle indicates signals belonging to the Li^+ -containing species, and the asterisk corresponds to folded resonances. For the experimental conditions, see Figure 2.

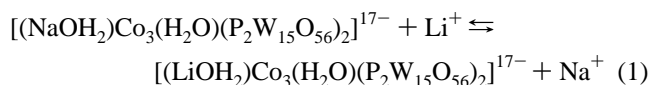
low temperature (see Figure 4, right part). At 274 K, the dynamic process is frozen, and four lines are observed corresponding to the P(2) signals from two different sandwich species. This phenomenon is fully reversible as the lines coalesce again when coming back to initial temperature.

Interestingly, because of the larger dispersion of the chemical shift for P(1), the NMR time scale is different, and the system is in the slow exchange process even at room temperature. This allows us to observe the four separate P(1) signals assigned to the two different sandwich species. According to the chemical shifts, the two external signals correspond to $\text{NaCo}_3\text{P}_4\text{W}_{30}$.

Observation of the coalescence of the P(1) signals would require us to increase the temperature, but this was accompanied by decomposition of the species. The respective proportion of the two species at various temperatures can be estimated from integration of the P(1) resonances. This shows that the new species is favored by an increase of the temperature. Moreover, at any given temperature, either 274 K (Figure 5), or 294 K (Figure 4, left), the concentration of the new species increases also with increasing $[\text{Li}^+]/[\text{Na}^+]$ ratio.

For example, at $[\text{Li}^+]/[\text{Na}^+] = 5.55$, the new species amounts are about 40% at 274 K and about 60% at 294 K (Figure 4).

All these observations suggest a lithium–sodium exchange in the sandwich cavity, according to equilibrium 1:



The same type of dynamic process was also observed for $[(\text{NaOH})_2\text{Co}_2(\text{P}_2\text{W}_{15}\text{O}_{56})_2]^{18-}$

(16) Jorris, T. L.; Kozik, M.; Casañ-Pastor, N.; Domaille, P. J.; Finke, R. G.; Miller, W. K.; Baker, L. C. W. *J. Am. Chem. Soc.* **1987**, *109*, 7402–7408.

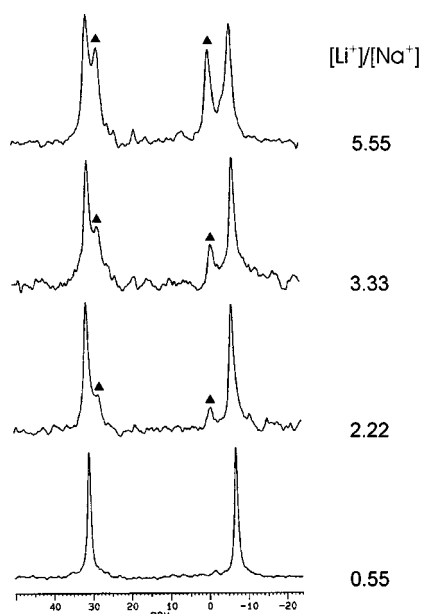


Figure 5. Low-frequency part (P(2) region) of the 121.5 MHz ^{31}P NMR spectra of $\text{NaCo}_3\text{P}_4\text{W}_{30}$ (0.02 M) in the presence of various concentration of LiCl. Temperature: 274 K. For the other experimental conditions, see Figure 2. The symbol ▲ indicates signals belonging to the Li^+ -containing species.

Preliminary Study of the Reactivity of 1 and 2. The di- and tricobalt complexes are formally unsaturated species. Addition of Co^{2+} to the aqueous solution of **1** and **2** induces the apparition of new signals in their respective ^{31}P NMR spectra. With 1 equiv of Co^{2+} added to $\text{Na}_2\text{Co}_2\text{P}_4\text{W}_{30}$, one obtains **2** ($\text{NaCo}_3\text{P}_4\text{W}_{30}$) as major compound with some amount of $\text{Co}_4\text{P}_4\text{W}_{30}$. On the other hand, addition of 1 equiv of Co^{2+} to $\text{NaCo}_3\text{P}_4\text{W}_{30}$ leads to the quantitative formation of one dissymmetrical $\text{Co}_4\text{P}_4\text{W}_{30}$ sandwich complex which evolves later in acidic medium into the symmetrical $\text{Co}_4\text{P}_4\text{W}_{30}$ form. These interconversion processes will be described in a forthcoming paper.

Electrochemistry. General Electrochemical Behavior. The electrochemical behavior of sandwich complexes of composition $[(\text{NaOH})_2\text{Co}_3(\text{H}_2\text{O})(\text{P}_2\text{W}_{15}\text{O}_{56})_2]^{17-}$ ($\text{NaCo}_3\text{P}_4\text{W}_{30}$, **2**) and $[(\text{NaOH})_2\text{Co}_2(\text{P}_2\text{W}_{15}\text{O}_{56})_2]^{18-}$ ($\text{Na}_2\text{Co}_2\text{P}_4\text{W}_{30}$, **1**) was mainly studied in aqueous solutions by cyclic voltammetry (CV). $\text{NaCo}_3\text{P}_4\text{W}_{30}$ and $\text{Na}_2\text{Co}_2\text{P}_4\text{W}_{30}$ complexes are stable in aqueous media between pH 0.5 and 6. Beyond this pH range, **1** and **2** become unstable because of hydrolytic decomposition.

These sandwich complexes exhibit at least three successive processes involving W in a negative potential range. In general, the reduction of heteropolyanions is accompanied by protonation at low pH; therefore, the pH of the solution has a great effect on the electrochemical behavior of the sandwich. For these three couples of oxo W-based reduction, the cathodic peak currents are almost proportional to the square root of the scan rate up to $100 \text{ mV}\cdot\text{s}^{-1}$ which indicates the electrode reaction of **1** and **2** to be diffusion controlled.

All electrochemical data at pH 2.52 are gathered in Table 2, and typical cyclic voltammograms are presented in Figures 6–8.

Table 2. Electrochemical Data of the Tetra-, Tri- and Dinuclear Dawson-Derived Sandwich Complexes^a

compound	W(1)	W(2)	W(3)
$\text{Co}_4\text{P}_4\text{W}_{30}$	-0.354 (2e, 60) -0.416 (2e, 66)	-0.534 (4e, 80)	-0.788 (2e, 74) -0.837 (2e, 94)
$\text{Na}_2\text{Co}_2\text{P}_4\text{W}_{30}$ (1)	-0.348 (2e, 44) -0.408 (2e, 56)	-0.529 (4e, 81)	-0.759 (2e, 94) -0.833 (2e, 71)
$\text{NaCo}_3\text{P}_4\text{W}_{30}$ (2)	-0.357 (2e, 54) -0.413 (2e, 54)	-0.537 (4e, 82)	-0.761 (2e, 82) -0.838 (2e, 67)
$\alpha\text{P}_2\text{W}_{15}$	-0.590 (4e) ^b -0.52 (4e) ^c	-0.812 (2e) ^b -0.78 (2e) ^c	

^a All redox potentials E° , approximated by $(E_p^a + E_p^c)/2$ for the reversible steps, are given in V vs SCE as obtained from cyclic voltammetry ($\nu = 20 \text{ mV}\cdot\text{s}^{-1}$) in Na_2SO_4 0.5 M + H_2SO_4 (pH 2.52). ^b In acetic acid–lithium acetate 0.1 M buffer, GC electrode. ^c In acetic acid–lithium acetate 1 M buffer, Hg electrode. Under bracket: (number of electron n , ΔE_p , peak splitting). ΔE_p is the difference potential between the oxidative and the reductive peak potentials.

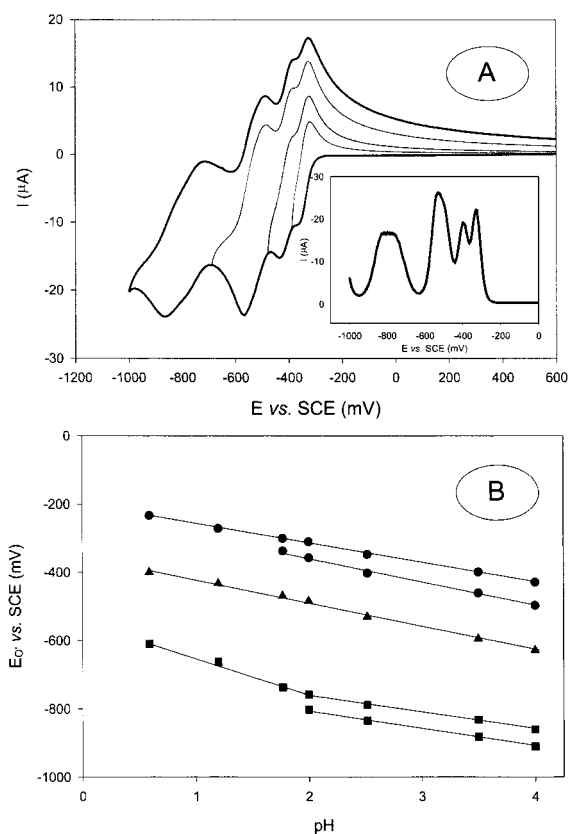


Figure 6. (A) Cyclic voltammograms of 1 mM $\text{NaCo}_3\text{P}_4\text{W}_{30}$ (**2**) in 0.5 M $\text{Na}_2\text{SO}_4 + \text{H}_2\text{SO}_4$ (pH 2.52) with different negative potential limits: -0.35, -0.42, -0.70, and -0.95 V. Scan rate $20 \text{ mV}\cdot\text{s}^{-1}$. Inset: differential pulse voltammetry at a scan rate of $25 \text{ mV}\cdot\text{s}^{-1}$. (B) Half-wave potential versus pH plots for the first (●), second (▲), and third (■) tungsten redox couples of $\text{NaCo}_3\text{P}_4\text{W}_{30}$ (**2**).

$\text{NaCo}_3\text{P}_4\text{W}_{30}$ (2**).** CVs of **2** in pH = 2.52 aqueous solutions are shown in Figure 6. $\text{NaCo}_3\text{P}_4\text{W}_{30}$ is stable in aqueous solution media between 0.5 and 6.0; nevertheless, the cyclic voltammogram is ill defined, and the peak current is much smaller for pH > 4. The same behavior was observed previously in the case of $\text{Co}_4\text{P}_4\text{W}_{30}$.⁷

At pH < 1.77, there are three well-defined redox processes in the negative potential range, between 0 and -0.95 V (Figure 6B). These three redox couples, originating from the tungsten oxo framework, are all four-electron reaction processes. With increasing pH, the redox potentials of these

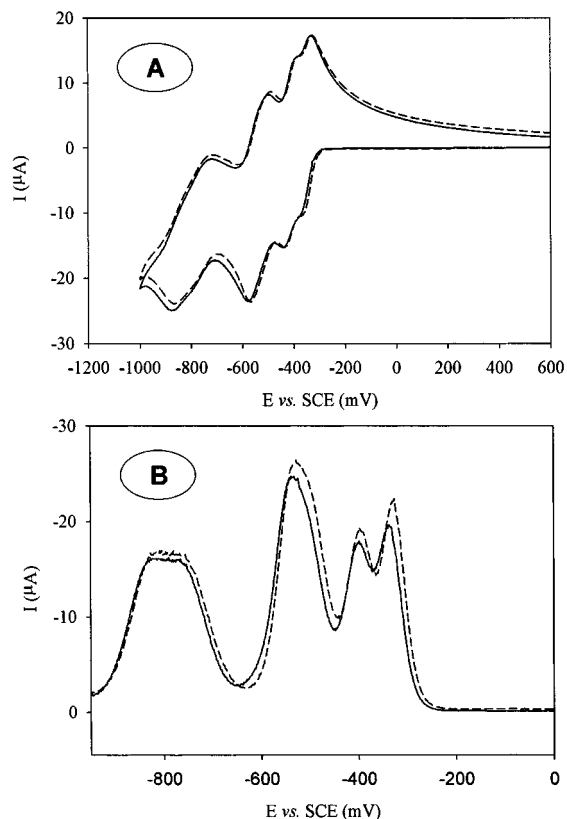


Figure 7. (A) Cyclic voltammograms of 1 mM $\text{Na}_2\text{Co}_2\text{P}_4\text{W}_{30}$ (**1**) and $\text{NaCo}_3\text{P}_4\text{W}_{30}$ (**2**) in 0.5 M $\text{Na}_2\text{SO}_4 + \text{H}_2\text{SO}_4$ (pH 2.52). Scan rate $20 \text{ mV}\cdot\text{s}^{-1}$. Full line: $\text{NaCo}_3\text{P}_4\text{W}_{30}$ (**2**). Dotted line: $\text{Na}_2\text{Co}_2\text{P}_4\text{W}_{30}$ (**1**). (B) Differential pulse voltammetry in 0.5 M $\text{Na}_2\text{SO}_4 + \text{H}_2\text{SO}_4$ (pH 2.52). Scan rate $25 \text{ mV}\cdot\text{s}^{-1}$. Full line: 1 mM **2**. Dotted line: 1 mM **1**.

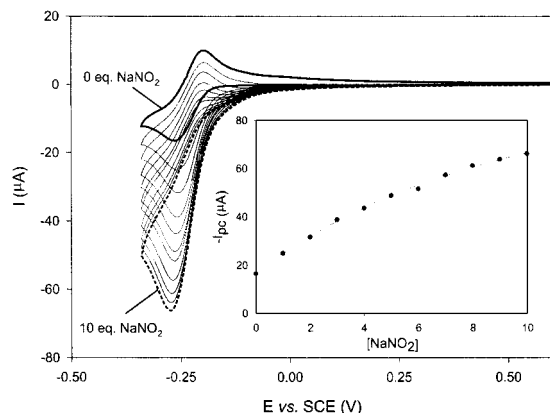


Figure 8. Cyclic voltammograms of 1.0 mM $\text{NaCo}_3\text{P}_4\text{W}_{30}$ in 0.5 M $\text{Na}_2\text{SO}_4 + \text{H}_2\text{SO}_4$ (pH 0.56), in the presence of various concentration of nitrite. Scan rate: $20 \text{ mV}\cdot\text{s}^{-1}$. The inset shows the variation of the catalytic current caused by the first cathodic wave vs concentration of nitrite.

three waves become more negative, and the first and the last four-electron waves split into two bielectronic waves (Figure 6A and Table 2).

However, the anodic-to-cathodic peak separation (ΔE_p) does not obey the classical voltammetry prediction where, at 25°C , $\Delta E_p = (59/n) \text{ mV}$ ($n = \text{number of electrons}$). For instance, at pH 2.52, the ΔE_p corresponding to the first bielectronic wave is between 44 and 56 mV ($> 30 \text{ mV}$), as shown in Table 2. This result suggests the presence of a very small splitting ($< 30 \text{ mV}$) of the first wave into two one-

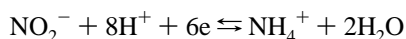
electron waves, too small to be observed by cyclic voltammetry or differential pulse voltammetry. Similar behavior was observed for the other waves.

The formal potentials of all three pairs of waves are dependent on pH, and the slopes of the formal potentials versus pH plots lie in the range 55–80 mV per pH unit between pH 1 and 4 (Figure 6B); this indicates that each added electron is accompanied by the addition of one proton to the reduced form of each redox couple. Controlled potential coulometry at -0.45 V versus SCE in a pH 2.52 media and under continuous bubbling and stirring consumes 4.2 electrons per molecule which shows that the first redox system exceeds a $2\cdot 2$ -electron process at $\text{pH} \geq 1.77$ (Figure 6).

In addition, one fourth reduction wave is observed in the more negative range, between -1.00 and -1.20 V . It is an irreversible multielectron wave which overlaps with the hydrogen evolution and is not shown on the figure. In the more positive potential range between $+1.60$ and -0.30 V , however, no redox waves are observed, suggesting that sandwich complex **2** has no electroactivity under our experimental conditions.

$\text{Na}_2\text{Co}_2\text{P}_4\text{W}_{30}$ (**1**). A similar behavior with only slightly different formal potentials was also observed for **1** (see Figure 7 and Table 2). Because the reduction potentials of $\text{Na}_2\text{Co}_2\text{P}_4\text{W}_{30}$ and $\text{NaCo}_3\text{P}_4\text{W}_{30}$ are similar, it is probable that the anions have analogous structures which remain intact as electrons are added.

Electrocatalysis of the NO_2^- Reduction. The reduction of nitrite to ammonia involves a six-electron–eight-proton change according to eq 2:



$$E^\circ (\text{vs. SCE at pH } 7) = 0.103 \text{ V} \quad (2)$$

However, direct electroreduction of nitrite ion requires a large overpotential at most electrode surfaces; otherwise, the photoreduction of NO_2^- can be catalyzed by nitrite reductase enzymes which are present in green plants. These enzymes consist of an iron–sulfur cubane unit associated with an iron siobacteriochlorin or a siroheme.^{17–18} Various transition metal complexes have been employed as enzymatic models for nitrite reduction, including iron chelate,¹⁹ iron²⁰ or cobalt²¹ porphyrin, or cobalt cyclam.²² Electroactive transition metals such as cobalt play an important role when they are coordinated to NO forming transition metal nitrosyl complexes as active sites.²³ They behave as key intermediates of the catalysis and are reduced by multiple-electron processes.

It has been shown that a large variety of oxometalates of Keggin or Dawson type are also efficient in the electrocatalytic reduction of nitrite and can be employed as enzymatic

- (17) (a) Losada, M. *J. Mol. Catal.* **1976**, *76*, 245. (b) Losada, M. *J. Electroanal. Chem.* **1979**, *104*, 205. (c) Candan, P.; Manzano, C.; Losada, M. *Nature* **1976**, *262*, 715.
 (18) Murphy, M.; Siegel, L. M.; Tove, S. R.; Kanin, H. *Proc. Natl. Acad. Sci. Am.* **1974**, *71*, 612.
 (19) Oyura, K.; Ishikawa, H. *J. Chem. Soc., Faraday Trans. 1* **1984**, *80*, 2243.

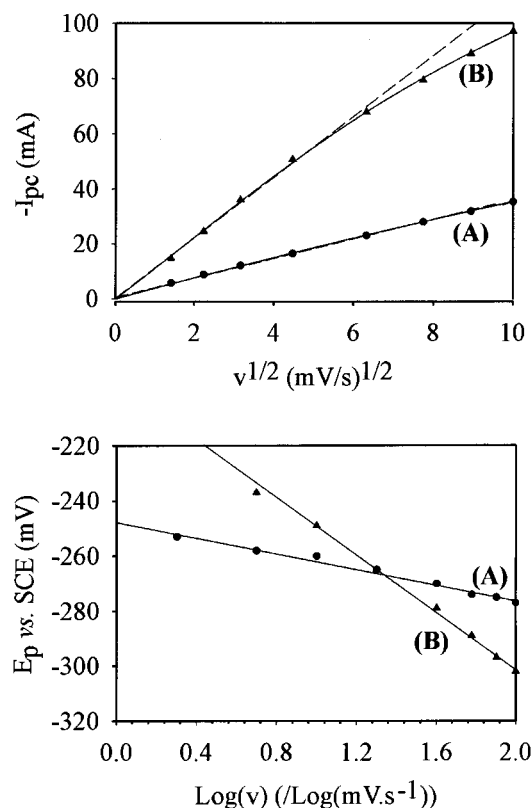


Figure 9. Top: plot of the peak current I_{pc} vs $v^{1/2}$ in 0.5 M $\text{Na}_2\text{SO}_4 + \text{H}_2\text{SO}_4$ (pH 0.56). (A) 1 mM $\text{NaCO}_3(\text{H}_2\text{O})\text{P}_4\text{W}_{30}$. (B) 1 mM $\text{NaCO}_3\text{P}_4\text{W}_{30} + 10$ mM NaNO_2 . Bottom: variation of the peak potential of the first cathodic wave as a function of the logarithm of scan rates.

models.^{1,24} It appeared that **1** and **2** could be good candidates for such a catalysis, and therefore, we decided to investigate their catalytic effect on the nitrite reduction.

Nitrous acid disproportionates slowly at low pH, which leads to the decreasing of the concentration of the active species (HNO_2 and NO) according to eq 3:^{24e}



Then, the catalytic effect decreases with waiting time, and therefore, the measurements have to be done immediately after the addition of the substrate.

At $\text{pH} < 3.5$, addition of NaNO_2 to the solution of **2** induces an increase of the cathodic peak current intensity of the first wave as shown in Figure 8. The inset shows that the cathodic current increases regularly with nitrite concentration.

- (20) (a) Barley, M. H.; Taheuch, K. J.; Meyer, T. J. *J. Am. Chem. Soc.* **1986**, *108*, 5876. (b) Barley, M. H.; Rhodes, M. R.; Meyer, T. J. *Inorg. Chem.* **1987**, *26*, 1746. (c) Younathan, J. N.; Wood, K. S.; Meyer, T. J. *Inorg. Chem.* **1992**, *31*, 3280.
 (21) Chang, S.-H.; Su, Y. O. *Inorg. Chem.* **1994**, *33*, 5847.
 (22) Tansguchi, I.; Nakoshima, N.; Matsushita, K.; Ysukouchi, K. *J. Electroanal. Chem.* **1987**, *224*, 199.
 (23) Richter-Addo, G. B.; Legzdins, P. *Metal Nitrosyls*; Oxford University Press: New York, 1992.
 (24) (a) Ayoko, G. A.; Olatung, M. A. *Ind. J. Chem.* **1984**, *23A*, 769. (b) Dong, S.; Lui, M. *J. Electroanal. Chem.* **1994**, *372*, 95. (c) McCornac, T.; Fabre, B.; Bidan, G. *J. Electroanal. Chem.* **1997**, *427*, 155. (d) Dong, S.; Xi, X.; Tian, M. *J. Electroanal. Chem.* **1995**, *385*, 227. (e) Belhourari, A.; Keita, B.; Nadjio, L.; Contant, R. *New J. Chem.* **1998**, *83*. (f) Toth, J. E.; Anson, F. C. *J. Am. Chem. Soc.* **1989**, *111*, 2444.

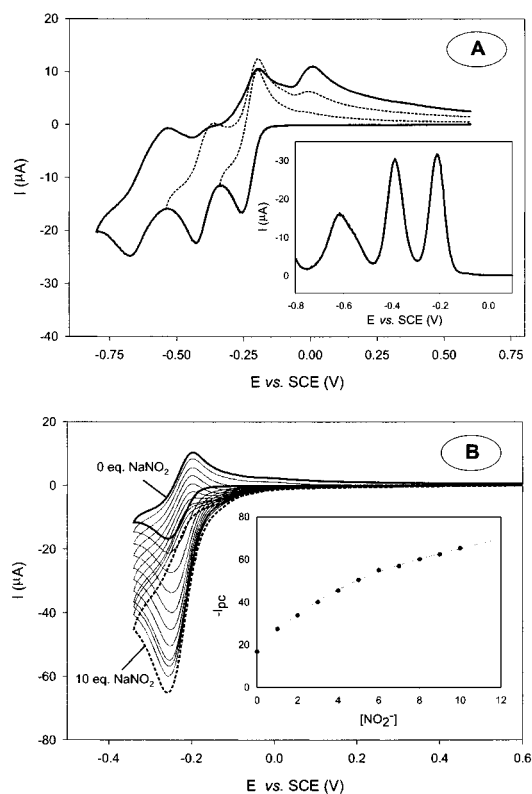


Figure 10. (A) Cyclic voltammograms of 1 mM $\text{Co}_4\text{P}_4\text{W}_{30}$ in 0.5 M $\text{Na}_2\text{SO}_4 + \text{H}_2\text{SO}_4$ (pH 0.56), with different negative potential limits: -0.30 , -0.55 , and -0.80 V. Scan rate $20 \text{ mV}\cdot\text{s}^{-1}$. Inset: differential pulse voltammetry. Scan rate $25 \text{ mV}\cdot\text{s}^{-1}$. (B) Cyclic voltammograms of 1.0 mM $\text{Co}_4\text{P}_4\text{W}_{30}$ in 0.5 M $\text{Na}_2\text{SO}_4 + \text{H}_2\text{SO}_4$ (pH 0.56), in the presence of various concentration of nitrite. Inset: plot of I_{pc} vs $[\text{NaNO}_2]$.

In contrast, the anodic current intensity decreases upon nitrite addition until the wave disappears completely: for example, at $\text{pH} = 0.56$, and with a scan rate of $20 \text{ mV}\cdot\text{s}^{-1}$, no reoxidation trace is found in the presence of more than 7 equiv of NaNO_2 .

Between 2 and $25 \text{ mV}\cdot\text{s}^{-1}$, the cathodic current is proportional to the square root of the scan rate, and the peak potential varies linearly with the logarithm of the scan rate, which implies a diffusion controlled catalytic process (Figure 9).

All these observations are consistent with electrocatalytic reduction of the nitrite anion.

The catalytic efficiency of the polyoxometalate (POM) is defined by $\text{CAT} = 100 \times (I_p(\text{POM}, \text{NaNO}_2) - I_p(\text{POM})) / I_p(\text{POM})$ where $I_p(\text{POM})$ and $I_p(\text{POM}, \text{NaNO}_2)$ are the cathodic peak currents in the absence and in the presence of NaNO_2 , respectively. As usually observed, the CAT increases with decreasing of the scan rate.

The influence of the pH was also investigated; for 1 mM $\text{NaCO}_3\text{P}_4\text{W}_{30}$ in the presence of 10 mM NaNO_2 , the catalytic efficiency, CAT, was 300%, 220%, 88%, 28%, and 0% at $\text{pH} = 0.59, 1.77, 2.52, 3.00$, and 3.50, respectively.

All these observations demonstrate that the active species must be essentially HNO_2 and not NO_2^- , at least up to $\text{pH} \approx 3$, according to the acidic equilibrium 4:



At $\text{pH} \geq 3.5$, no catalytic effect is observed for any of the three reduction processes of $\text{NaCo}_3\text{P}_4\text{W}_{30}$. In this medium, the nitrite anion predominates, and this behavior is in agreement with a charge repulsion between the two anionic species, that is, NO_2^- and the 17^- charged polyoxotungstate.

A similar electrocatalytic behavior is also observed for $\text{Na}_2\text{Co}_2\text{P}_4\text{W}_{30}$ or $\text{Co}_4\text{P}_4\text{W}_{30}$ (Figure 10).

Summary and Concluding Remarks

In this work, we report for the first time the preparation and the characterization of two novel di- and trinuclear sandwich complexes of composition $[(\text{NaOH}_2)_2\text{Co}_2(\text{P}_2\text{W}_{15}\text{O}_{56})_2]^{18-}$ and $[(\text{NaOH}_2)\text{Co}_3(\text{H}_2\text{O})(\text{P}_2\text{W}_{15}\text{O}_{56})_2]^{17-}$.

The electrochemical behaviors of $\text{NaCo}_3\text{P}_4\text{W}_{30}$ and $\text{Na}_2\text{Co}_2\text{P}_4\text{W}_{30}$ compounds were investigated systematically at various pHs, by reference to that of $\text{Co}_4\text{P}_4\text{W}_{30}$. All these compounds exhibit three reversible W-centered reduction processes with slightly different peak potentials, which strongly suggests that the anions have analogous structures and that these structures remain intact as electrons are added.

These results, associated with the recent reports of Hill

and coworkers,⁶ lead us to propose that the “lacunary” sandwiches $[(\text{NaOH}_2)_2\text{Fe}^{\text{III}}_2(\text{P}_2\text{W}_{15}\text{O}_{56})_2]^{16-}$, $[(\text{NaOH}_2)_2\text{Co}_2(\text{P}_2\text{W}_{15}\text{O}_{56})_2]^{18-}$, and $[(\text{NaOH}_2)\text{Co}_3(\text{H}_2\text{O})(\text{P}_2\text{W}_{15}\text{O}_{56})_2]^{17-}$ are the first members of two large classes of di- and trimetallic polytungstates deriving from a trivacant precursor. Additional members of these new classes of polytungstates will be likely synthesized in the near future. This opens the route to the preparation of mixed-metal sandwich complexes, with expected catalytic and magnetic properties. Current work on this topic is in progress, and new results will be reported soon.

Acknowledgment. This research was supported by the CNRS and by the Universities Paris XI (Université Paris-sud Orsay) and Paris VI (Université Pierre et Marie Curie). We thank Professor Louis Nadjó (Orsay) for critical reading of the manuscript, Martine Richet for the chemical analysis, and Guillaume Genet for some of the electrochemical measurements.

IC020146U